Journal of Cleaner Production 467 (2024) 142968

Contents lists available at ScienceDirect

Journal of Cleaner Production

journal homepage: www.elsevier.com/locate/jclepro

Exergy, energy, performance, and combustion analysis for biodiesel NO_x reduction using new blends with alcohol, nanoparticle, and essential oil

Arun Teja Doppalapudi [a], Abul Kalam Azad [a,*], Mohammad Masud Kamal Khan [b]

[a] School of Engineering and Technology, Central Queensland University, 120 Spencer Street, Melbourne, VIC, 3000, Australia
[b] School of Engineering, Computer & Mathematical Sciences, Auckland University of Technology, Auckland, New Zealand

ARTICLE INFO

Handling Editor: Cecilia Maria Villas Bôas de Almeida

Keywords:
Biodiesel
NO_x emissions
Fuel modifications
Carbon nanotube
Fuel exergy
Fuel energy

ABSTRACT

Biodiesel is considered one of the alternative replacements to fossil fuels. However, the major challenge associated with its application in diesel engines is the higher level of NO_x emissions. Fuel modification technologies, where biodiesel is blended with various additives and fuels, have emerged as a distinguished method in recent years to improve engine performance and reduce NO_x. The study aims to reduce NO_x emissions by fuel modification techniques. Five blends were prepared using Tucuma biodiesel along with ethanol, carbon nanotubes, and eucalyptus oil. The prepared blends were deployed to a test bed engine at rated speed and by varying loads to investigate performance, emission, and combustion characteristics. The results revealed that ethanol-blended fuels such as DE10 and TB10E10 had reduced the NO_x emissions by 51.37% and 9%, respectively, at lower loads compared to diesel. Although the nanoparticle blend exhibited increased NO_x emissions compared to diesel, it demonstrated reductions of 4.1%, 4.56%, 7.2%, and 3.1% at loads of 25%, 50%, 75%, and 100%, respectively, compared to TB10. The study highlights various tradeoffs observed between operating conditions and engine parameters for the blends, as detailed in this research. The study found that blends TB10E10 and TB10E10CNT20 exhibit improved performance close to that of diesel and reduced NO_x and CO emissions compared to that of diesel and TB10. The study recommends further exploring the impact of injection rates with ethanol-blended fuels as they showed longer ignition delays since advancing the injection can create better combustion with ethanol blends.

Abbreviations

ASTM	American Society for Testing and Materials
BSFC	Break-specific fuel consumption
BMEP	Brake mean effective pressure
BP	Brake power
BTE	Brake thermal efficiency
CO	Carbon monoxides
CD	Combustion duration
CNTs	Carbon nanotubes
DE10	Diesel 90%+Ethanol 10%
EGT	Exhaust gas temperature
FAME	Fatty acid methyl esters
HC	Hydrocarbons
HRR	Heat release rate
ID	Ignition delay
KOH	Potassium hydroxide
MFB	Mass fraction burnt
MWCNTs	Multi-walled carbon nanotubes
NO	Nitrogen monoxide
NO_x	Nitrogen oxides
RSM	Response surface methodology
TB10	Tucuma 10%+ Diesel 90%
TB10E10	Tucuma biodiesel 10% + Ethanol 10% +Diesel 80%
TB10E10CNT20	Tucuma 10% + Ethanol 10% +Diesel 80%+CNTs 20 ppm
TB10E10Eu10	Tucuma 10% + 10% Ethanol +10% Eucalyptus +70% diesel by volume
TDC	Top dead center

1. Introduction

Biodiesel has shown better replacement for fossil fuels in diesel engines (Azad et al., 2024). Considering higher carbon emissions from fossil fuels, biodiesel can be an alternative energy source in the marine,

* Corresponding author.
E-mail addresses: a.doppalapudi@cqu.edu.au (A.T. Doppalapudi), a.k.azad@cqu.edu.au (A.K. Azad).

https://doi.org/10.1016/j.jclepro.2024.142968
Received 19 March 2024; Received in revised form 7 June 2024; Accepted 19 June 2024
Available online 20 June 2024

transportation, and agricultural sectors to reduce greenhouse gas emissions (Towoju, 2022). Recent research revealed that biodiesel reduces about 78% of net carbon emissions compared to fossil fuel on its lifecycle (Atadashi et al., 2010b; Gerpen, 2005). It also lowers emissions such as carbon monoxide (CO), hydrocarbon (HC), sulfates, particulate matter (PM), polycyclic aromatic hydrocarbons, and nitrated polycyclic aromatic hydrocarbons (Balat and Balat, 2010; Doppalapudi et al., 2021). However, the primary concern with biodiesel is the elevated levels of NO_x emissions in comparison to those generated by fossil fuels. The higher NO_x emissions can impact human health and the environment (Boningari and Smirniotis, 2016). For instance, nitrogen oxides diffuse through the respiratory organs and disrupt the alveolar structures and their function in the lungs (Sperber, 2012; Li et al., 2018). NO_x emissions also impact the environment, promoting the formation of photochemical smog, acid rain, and ozone depletion (Guo et al., 2022). Hence, reducing the NO_x from biodiesel is one of the critical aspects that needs to be addressed.

Biodiesel properties, including higher density, viscosity, and bulk modulus, significantly influence NO_x emissions and contribute to higher fuel consumption (Azad et al., 2023a; Köse et al., 2021). At the same injection duration, Szybist et al. (2007) observed more fuel consumption with biodiesel than diesel because of higher bulk modulus. Compared to diesel, biodiesel has a 12% lower energy content (lower heating value) and is responsible for increased fuel consumption by 2%–10% to achieve the rated power(Atabani et al., 2012; Balat and Balat, 2010). For instance, Gharehghani et al. (2019) revealed an increased break-specific fuel consumption (BSFC) for Waste fish oil blend and higher NO_x at the same condition (Gharehghani et al., 2017). Also, biodiesel contains 10%–12% oxygen in its structure, contributing to increased NO_x emissions (Atadashi et al., 2010a; Knothe, 2010; Demirbas, 2007). According to Zeldovich's mechanism, NO_x, specifically nitrogen monoxide (NO), is formed at elevated temperatures, where nitrogen in the air reacts with oxygen and forms NO (Rajak et al., 2020). Air contains 78% nitrogen and 21% oxygen, and further adding biodiesel oxygen percentage to the total combustion will cause higher NO_x with biodiesel than diesel (Hao et al., 2021). Other factors such as higher cloud points, cetane index, and pour points of the biodiesel fuels are also responsible for the higher NO_x due to reduced ignition delay and cold start conditions (Tong et al., 2011; Jena et al., 2010). The fuel properties vary depending on the feedstock type, and several authors have researched blending biodiesel with other oxygenated fuels to reduce harmful NO_x emissions (Elkelawy et al., 2019; Shahir et al., 2015a). For example, Rahman et al. (2018), blended orange oil with diesel, noticed an increased heating value of the total blend, and reported reduced NO_x. In another study, Rahman et al. (2019) observed that the Eucalyptus-diesel blend showed reduced NO_x compared to the orange oil-diesel blend at full load conditions. Recent studies also revealed that adding essential oils has affected the fuel's physiochemical properties and impacted NO_x emissions (Butkus et al., 2007; Purushothaman and Nagarajan, 2009). Furthermore, adding alcohols (oxygenated fuels) is one of the methods to improve the biodiesel blend's physical properties and reduce NO_x emissions (Azad et al., 2016; Rahman et al., 2017).

Ethanol is widely used as a transportation fuel due to its low viscosity and good cold-flow properties (Wei et al., 2018; Datta and Mandal, 2017; Hulwan and Joshi, 2011; Halder et al., 2019). For instance, Paul et al. (2017) reported that The addition of 15% ethanol to Pongamia biodiesel resulted in decreased viscosity and demonstrated improved fuel atomization, leading to higher in-cylinder pressure and a higher heat release rate (HRR). Ethanol contains approximately 34% oxygen content by weight and can be produced from renewable sources (Mirhashemi and Sadrnia, 2020). The lower heating value of the ethanol escalates fuel vaporization inside the chamber and reduces the combustion temperatures (Shahir et al., 2015b; Ashok et al., 2019). According to Vergel-Ortega et al. (2021), there was a decrease in NO_x by 5% and 8.3% when the ternary blend (palm, sunflower oil, and diesel) was mixed with 2% and 4% ethanol. In addition, Guarieiro et al. (2009) observed a decrease in NO_x emissions by 30% and 84% at 1800 rpm and 2000 rpm with the addition of 10% ethanol to the diesel blend. Several studies revealed that decreased NO_x emissions are possible with the biodiesel and ethanol blends (Wei et al., 2018; Datta and Mandal, 2017; Saleh and Selim, 2017; Alptekin et al., 2015; Zhu et al., 2010a; Yilmaz and Sanchez, 2012; Yilmaz et al., 2014; Shanmugam et al., 2011; Ferreira et al., 2013). However, some studies have shown increased NO_x emissions with the biodiesel and ethanol blends (Emiroğlu and Şen, 2018; Alptekin, 2017; Hulwan and Joshi, 2011; Turkcan, 2018; Shi et al., 2005; Shi et al., 2006; Barabas et al., 2010). There is a delicate tradeoff with the combustion parameters that affect the NO_x emissions with ethanol-biodiesel blends. On the other hand, adding nanoparticles to biodiesel fuels has improved the combustion rates, revealed better performance and reduced NO_x (Annamalai et al., 2016; Basha and Anand, 2011, 2014; Banapurmath et al., 2014).

Carbon nanotubes (CNTs) as additives to biodiesel have improved combustion characteristics due to their high thermal conductivity and high energy density (Zhu et al., 2010b). For instance, Heydari-Maleney et al. (2017) it investigated the effect of CNTs on biodiesel blends. This study reported an increase in brake thermal efficiency (BTE) by 13.97% and reduced the CO, HC and soot emissions by 5.47%, 31.72%, and 6.96%, respectively. El-Seesy et al. (2017) conducted engine tests with Jatropha biodiesel by blending it with CNTs, and the study reported that a dose level of CNTS with 20 mg/l with Jatropha B20 has reduced NO_x, CO, and UHC by 35%, 50%, and 60%, respectively (El-Seesy et al., 2017).

Much work has been done on biodiesel-ethanol blends; still, there is limited useful literature comparing the NO_x emission reduction among modified blends. The novelty of this study lies in its comprehensive comparison of different modified biodiesel blends and their effectiveness in reducing NOx emissions. The study specifically examines biodiesel blends by blending the biodiesel with ethanol, carbon nanotubes, and eucalyptus oil offering a unique perspective on how these additives interact and influence emission characteristics. The study has chosen a 10% ethanol blend ratio as suggested by the authors Khoobbakht et al. (2016) and Vergel-Ortega et al. (2021). From the experimental studies conducted by Hosseini et al. (2017), Suresh et al. (2023) and Venkatesan et al. (2023), NO_x emissions were found to increase with the increase in CNTs concentrations in the blend. The experimental tests conducted by Najafi and Shadidi (2024) and Solmaz et al. (2021) with CNT 25 ppm and Murugesan et al. (2023) with CNT 20 ppm as additives to the biodiesel showed reduced NO_x compared to the higher quantities of CNT concentrations in the blend. Hence, CNTs at 20 ppm were added to the biodiesel-ethanol blend to study the effects of combustion variations in diesel engines to reduce NO_x. Moreover, pure eucalyptus oil (10% by volume) is added to the biodiesel ethanol blend to examine the impact of fuel oxygen content on NO_x emissions. The study has extracted some valuable conclusions from the blends by incorporating combustion patterns, fuel exergy, and energy analysis into NO_x emissions.

2. Materials and methods

2.1. Materials

This study investigated the impact of various biodiesel blends and additives on diesel engine performance, emission, and combustion. The following is the detailed list of materials utilized in the study. Tucuma bio-oil was acquired from a USA-based supplier, Nature In Bottle, and it was converted to biodiesel using a transesterification process. High-grade potassium hydroxide (KOH) and methanol were obtained from Westlab Pty. Ltd. Australia to conduct the transesterification reaction. In addition, blue gum Eucalyptus is purchased from Australian Wholesale Oils to prepare the blends. Furthermore, multi-walled nanotubes (outside diameter ~10–20 nm) with 99% purity were obtained from the Carb lab tech supplies for the blend preparation. Furthermore, ethanol is supplied by local supplier Sydney Solvents and diesel fuel is obtained

from the Ampol Petroleum Company and used for engine operations and biodiesel blend preparations.

2.2. Biodiesel conversion and blend preparation method

Tucuma bio-oil is converted to biodiesel using the transesterification process (Bhuiya et al., 2015; Azad, 2017). To achieve higher yields, the transesterification reaction was carried out in optimized conditions using the response surface methodology (RSM) technique. The RSM technique, coupled with the Box- Behnken design, is generated to record high-order responses using four parameters: time, temperature, catalyst concentration, and methanol ratio. A total of 27 test runs were conducted to optimize these four parameter references, and an optimized condition was recorded at 7:1 methanol to oil molar ratio, 0.5% (w/w) KOH catalyst amount, 70 min reaction time, and 53 °C temperature conditions. After the reaction, glycerol was separated from the mixture, and the remaining biodiesel was water-washed using demineralized water. The washed biodiesel was then heated at 110 °C to remove any water particles present in the fuel, and finally, the pure biodiesel was extracted with 99.6% yield at the optimized condition.

The fatty acid methyl esters (FAME) analysis is carried out as per AOCS Ce 1a-13 standards using gas chromatography (GC) and mass spectrometry testing equipment. The GC test results show the Tucuma biodiesel contains mainly oleic (44.87%), palmitic (25.69%), linoleic (12.56%), and stearic (11.8%) fatty acids. The physicochemical properties of pure biodiesel samples were tested by following the corresponding American Society for Testing and Materials (ASTM) standards and are presented in Table 1.

Five blends were prepared by varying the blend percentages and keeping the baseline fuel as diesel. All the blends were prepared in percentage volume that means DE10 (10% Ethanol + 90% diesel by volume), TB10 (10% Tucuma +90% diesel by volume), TB10E10 (10% Tucuma +10% Ethanol + 80% diesel by volume), TB10E10CNT20 (10% Tucuma +10% Ethanol + 20 ppm of CNTs + 80% diesel by volume) and TB10E10Eu10 ((10% Tucuma +10% Ethanol +10% Eucalyptus + 70% diesel by volume). The diesel, biodiesel, and ethanol blends were prepared in a batch of 4 L using a 5-L conical flask with the help of a magnetic stirrer. Except for the CNTs blend mixture, all the blends were stirred for 60 min by maintaining stirrer speed at 500 rpm with temperatures ranging around 26 ± 1.5 °C. The blends were stored in closed containers for 12 h to verify the layer separation and no layer separation was recorded. In the case of CNTs, intense blends were prepared overnight by maintaining the stirrer speed at 700 rpm and used promptly to avoid any settling of CNTs in the blend. The physicochemical properties of the prepared blends were also presented in Table 1.

2.3. Engine experiment setup and test details

Fig. 1 illustrates the schematic representation of the engine test rig operated by the data acquisition system. The engine tests were performed on a 4-cylinder, four-stroke Kubota V3300 commercial engine and the technical specifications are presented in Table 2. The engine was connected to an eddy current dynamometer, which was used as the loading device. Engine torque, speed, and mass flow rates are measured during the test, and the engine performance parameters, including brake power (BP), brake thermal efficiency (BTE), brake specific fuel consumption (BSFC), and brake mean effective pressure (BMEP), were evaluated using standard equations. A standalone piezoelectric pressure transducer (H32218-GPA, Optrand, MI, USA) was mounted on the cylinder head to gauge the pressure inside the chamber. The pressure was recorded as the average of a hundred consecutive cycles (cycle refers to 0 ^{o}CA to 720 ^{o}CA) and was delivered with respect to the degree crank angle. The emissions were measured using a CODA (Andros 6241A, California, USA) exhaust gas analyzer. The equipment uses nondispersive infrared technology and measures emissions such as CO, CO_2, HC, and NO_x accurately and instantaneously. The measuring range and accuracy of the instrument are detailed in Table 2.

The test experiments were carried out using the SAE J1995 engine test standard, where the engine was kept operated at a constant speed of 2400 rpm, and the load were varied as 25%, 50%, 75%, and 100% load. The engine was kept running for 10 min in each test condition before the data was recorded to ensure its stability. After each run, the leftover fuel was pumped out from the tank, and new fuel was sent to the cylinder. At least three sets of data were recorded for each operating condition of the experiment at different time intervals to ensure the precision of the recorded data.

2.4. Associated theories and equations

The following performance and combustion parameters are used for the analysis.

1) Brake power (BP) is the power accessible at the engine shaft output, and the engine BP can be calculated using equation (1) (Odibi et al., 2019).

$$BP = \frac{2\pi NT}{60 \times 1000} \quad (kW) \tag{1}$$

Where BP is in kW, T is the engine's torque in N.m, and N is the engine speed in rpm.

Table 1
Fuel properties of Tucuma biodiesel fuels as per ASTM standards.

Property	Test reference	Tucuma biodiesel	ASTM D6751 standard biodiesel	Diesel	DE10 blend	TB10 blend	TB10E10 blend	TB10E10CNT20 blend	TB10E10Eu10 blend
Density (15 °C) in kg/m^3	ASTM D1298	879.1	860–890	832	870.19	874.39	865.2	865.48	868.87
Viscosity (40 °C) in mm^2/s	ASTM D445	4.0	1.9–6.0 mm^2/s	4.1	3.71	4.01	4.04	4.04	3.64
Calorific value in MJ/kg	ASTM D240	39.87	–	41.77	40.293	41.58	43.4446	43.439387	37.711
Cetane index	ASTM D613	48.2	Min^m 47	44	–	–	–	–	–
Flashpoint (°C)	ASTM D93/ IP 34	186	Min^m 100	62	43.38	47.78	46.82	46.81	42.54
Acid value (mgKOH/g)	ASTM D664	0.47	–	–	–	–	–	–	–
Carbon %		85.10		76.59	81.80	84.25	87.76	87.77	80.14
Oxygen %		0.00		0	3.47	1.24	4.71	4.71	5.84
Hydrogen %		14.80		11.05	14.63	14.43	15.44	15.44	13.95
O/C		0.00		0.16	0.04	0.01	0.05	0.05	0.07
H/C		0.17		0.14	0.18	0.17	0.18	0.18	0.17

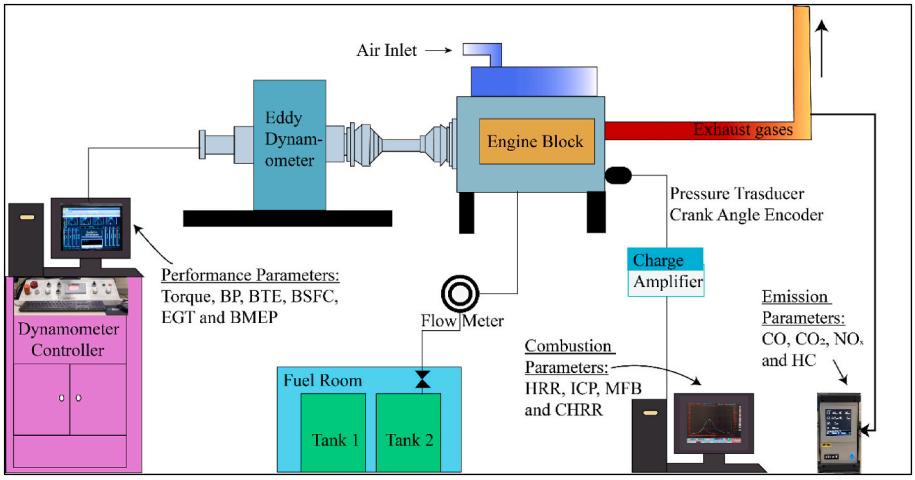

Fig. 1. Engine test setup and testing instruments.

Table 2
Specification of the engine with an eddy current dynamometer and emission analyzer.

Engine Specification		Accuracy of emission analyzers	
Engine model	Kubota V3300	Parameter (range)	Accuracy
Type	Vertically water-cooled	O_2 (0–25%vol)	±0.1 % abs
Number of cylinders	4	NO_x (0–5000 vol ppm)	±20 ppm ab
Bore x stroke (mm)	98 x 110	HC (0–3000 ppm vol)	±4 ppm ab
Total displacement and compression ratio	0.003318 m^3 and 22.6:1	CO (0–15%vol)	±0.02 % abs
Injection timing and injection pressure	16 ^{0}CA BTDC and 13.73 Mpa	CO_2 (0–20%vol)	±0.3 % abs

2) Brake thermal efficiency (BTE) is the amount of work produced from the fuel energy supplied and is estimated from equation (2) (Nabi et al., 2019b).

$$BTE = \frac{BP}{m_f \times Fuel\ calorific\ vale}\ (\%) \tag{2}$$

Where m_f is the mass flow rate of the fuel in kg/hr.

3) Brake-specific fuel consumption (BSFC) is the fuel consumption rate with respect to engine power, and it can be calculated using equation (3) (Odibi et al., 2019).

$$BSFC = \frac{m_f}{BP}\ (kg/kW.h) \tag{3}$$

4) Brake mean effective pressure is estimated from equation (4).

$$\mathrm{BMEP} = \frac{BP \times 60}{L \times V \times \left(\frac{N}{n}\right) \times No.\ of\ cylinders \times 100}\ (bar) \tag{4}$$

Where L denotes the stroke length (m), V represents the piston volume (m^3), N is the rotational speed, and n is 2 for four-stroke engines.

5) The in-cylinder heat release rate (HRR) is determined from the pressure values utilizing the first law of thermodynamics, as represented in equation (5) (Kishore et al., 2024; Azad et al., 2023b; Nabi et al., 2019a).

$$\frac{dQnet}{d\theta} = \frac{\gamma}{\gamma - 1} p \frac{dV}{d\theta} + \frac{1}{\gamma - 1} v \frac{dP}{d\theta} \left(\frac{J}{^\circ CA}\right) \tag{5}$$

Where Q_{net} represents HRR (J/°CA), γ is the ratio of specific heats, p denotes the in-cylinder pressure at the given crank angle (Pa), and v represents the in-cylinder volume in (m^3).

6) Mass fraction burnt (MFB) inside the cylinder helps to identify the start and finish of the combustion, and it can be calculated using equation (6) (Mendera et al., 2002; Yin et al., 2023).

$$MFB = \frac{\sum_0^i \Delta_P}{\sum_0^n \Delta_P} \tag{6}$$

where Δ_P is the pressure rise during the combustion, and "n" is the number of crank angle intervals between the start and finish of combustion.

2.5. Energy and exergy analysis

2.5.1. Fuel energy analysis

In this analysis, the energetic efficiency and energy loss will be determined by the balance of input and output masses and energies in a control volume system. Using the first law of thermodynamics, the steady state of a system is presented in equation (7).

$$Energy_{in} = Energy_{out} \tag{7}$$

In a diesel engine, the input energy amount of fuel energy supplied and has been expanded in equation (8).

$$E_{in} = \dot{m}_f \times LHV_f \tag{8}$$

Where $\dot{m}_f$ is the mass of the fuel, and LHV is the calorific value of the fuel

The generated power is primarily intended for power generation purposes. Any outputs other than power generation are categorized as losses. The output energy produced is distributed among brake power, cooling water system, exhaust gases and unaccounted losses. The unaccounted energy is the loss, which is any output other than the power generated. The output energy is expressed in equation (9).

$$E_{out} = E_{BP} + E_{cw} + E_{eg} + E_{unaccounted} \tag{9}$$

Where E_{BP} is the shaft power can be calculated using Equation 10

$$E_{BP} = \frac{2 \times \pi \times N \times T}{60,000} \tag{10}$$

Where N is the speed in rpm, T is the engine torque in N.m.

The heat energy distributed to the cooling water (E_{cw}) and exhaust gases (E_{eg}) is calculated using equations (11) and (12).

$$E_{cw} = \dot{m}_a \times C_{p\,(w)} \times \Delta T \tag{11}$$

Where $\dot{m}_a$ is the mass flow rate of the cooling liquid and CP_w is the heat capacity of the coolant liquid, and ΔT is the difference between the inlet and output temperatures of the cooling pipe.

$$E_{eg} = \left(\dot{m}_a + \dot{m}_f\right) \times C_{p\,(eg)} \times \Delta T \tag{12}$$

Where $CP_{(eg)}$ is the heat capacity of the coolant liquid.

2.5.2. Exergy analysis

The quality of the energy transfer can be characterised using the exergy analysis (Krishnan and Rajkumar, 2022). Exergy is the energy a system possesses, and the exergy balance can be calculated using equation (13) for the given control volume.

$$Exergy_{in} - Exergy_{out} = Ex_{destruction} \tag{13}$$

$Exergy_{in}$ is the input exergy from the fuel and can be calculated using equation (14) (Nabi et al., 2020).

$$Exergy_{in} = \dot{m}_f \times LHV_{fuel} \times Exergy_{chem} \tag{14}$$

where, $Exergy_{chem}$ is the chemical exergy associated with the fuel, which was determined using equation (15) (Odibi et al., 2019).

$$Ex_{chem} = 1.0401 + 0.1729\left(\frac{H}{C}\right) + 0.0432\left(\frac{O}{C}\right) + 0.2169\left(\frac{S}{C}\right) \times \left(1 - 20628\left(\frac{H}{C}\right)\right) \tag{15}$$

2.6. Uncertainty analysis

Verifying measured data uncertainty involves evaluating both the uncertainty of the measuring equipment and the system's accuracy. Various factors contribute to uncertainties, such as instrument malfunctions, calibration inaccuracies, test environment conditions (whether steady-state or unsteady-state), testing methodologies, and data interpretation. The total uncertainty accounts for the combination of all individual uncertainties related to the parameters under investigation. The overall percentage of uncertainty was determined using equation (16) (Sharma and Murugan, 2015; Mosarof et al., 2016; Manimaran et al., 2023; Venu et al., 2022; Azad et al., 2023b).

$$U_o = \sqrt{U_{FC}^2 + U_{BSFC}^2 + U_{BTE}^2 + U_{HC}^2 + U_{CO_2}^2 + U_{CO}^2 + U_{NO_x}^2 + U_{\lambda}^2 + U_{Exergy}^2 + U_{energy}^2 + U_{HRR}^2}$$
$$= \sqrt{(0.10)^2 + (0.70)^2 + (0.90)^2 + (0.30)^2 + (0.02)^2 + (0.80)^2 + (0.10)^2 + (0.8)^2 + (0.0.6)^2 + (0.9)^2 + (0.05)^2} = \pm 1.8\% \tag{16}$$

3. Results and discussions

3.1. Emission analysis

3.1.1. Effect of NO_x emissions concerning loads

Fig. 2 illustrates the percentage increase and decrease in NO_x emissions compared to diesel fuel. The difference in NO_x emission rates is

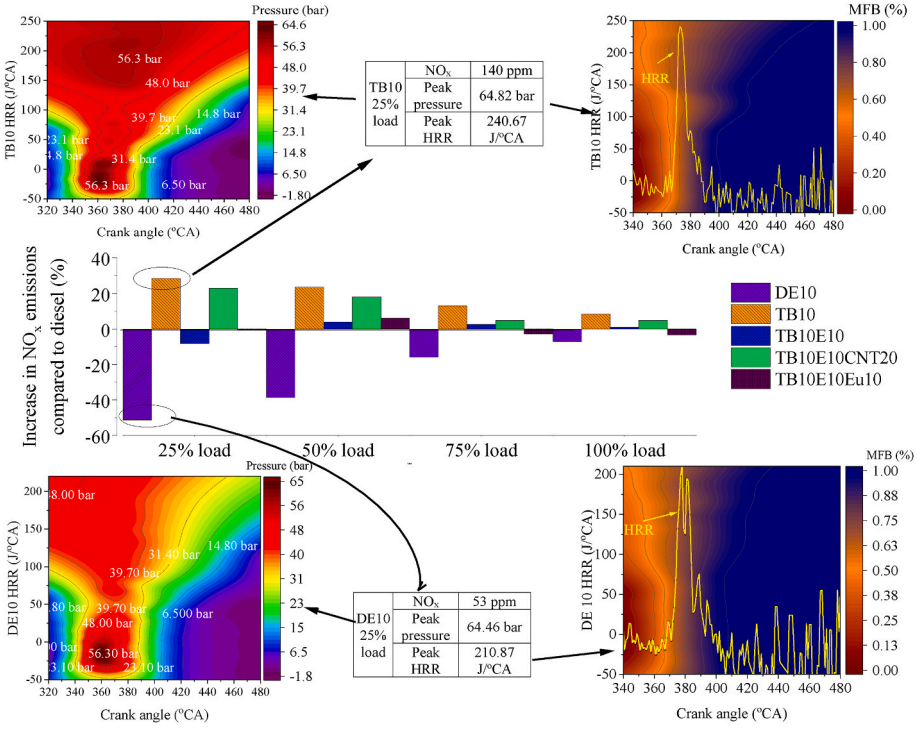

Fig. 2. Variation of NO_x emissions with respect to loads correlates with HRR and MFB combustion parameters at lower load conditions.

higher between low and high loads. Mainly, Fig. 2 highlights the cylinder pressure and MFB contours of DE10 and TB10 at 25% load as they have shown higher and lower NO_x than diesel and other blends. At 25% loads, the highest decrease in NO_x is noted with DE10 (51.37%), followed by TB10E10 (9%) and TB10E10Eu10(1%), respectively. The TB10 and TB10E10CNT20 showed increased NO_x by 28.4% and 23%, respectively, compared to diesel. It is because the in-cylinder thermal state is poor at low loads, and combustion efficiency decreases (Ma et al., 2024; Pedrozo et al., 2016). The MFB plots show higher mass fractions are noticed for TB10 than DE10 MFB. Fig. 2 shows higher peak HRR and pressure values are noted for TB10 compared to DE10; this indicates that unregulated rapid combustion occurs at a lower load with a biodiesel blend. Hence, TB10 showed higher NO_x compared to all other fuels at lower loads. Besides, adding ethanol to the TB10 has decreased the NO_x compared to normal TB10. The main reason behind this is the presence of ethanol, which has created a cooling effect inside the chamber and reduced NO_x (Shahir et al., 2015b). Because of the high latent heat of vaporization, ethanol absorbs heat from the chamber during fuel atomization and vaporization, reducing the combustion temperatures (Paul et al., 2016, 2017). Similar results were also noted by Guarieiro et al. (2009), He et al. (2003) and Agarwal (2007). Followed by TB10; TB10E10CNT20 showed higher NO_x at all loads. Though the addition of CNTs showed reduced NO_x compared to TB10, the emissions are higher with the ethanol blend TB10E10. For example, Elkelawy et al. (2023) observed a decrease in NO_x by adding CNTs to the biodiesel blends (B40) compared to their respective normal biodiesel blends test runs. Moreover, less NO_x is also noticed when Eucalyptus oil is added to the blend. This is mainly due to the lower heat release (refer to HRR graph Fig. 10) rates caused by poor combustion. The lower calorific value (as per Table 1) of the blends have caused lesser heat release rate (Devan and Mahalakshmi, 2009).

A higher magnitude of NO_x is observed at higher loads, as shown in Fig. 3. The higher NO_x is observed for TB10 (315 ppm), followed by TB10E10CNT20 (305 ppm), TB10E10 (294 ppm), diesel (291 ppm), TB10E10Eu10 (281 ppm) and DE10 (270 ppm). Higher NO_x at high loads is mainly due to the difference in the thermal state of the in-cylinder atmospheric conditions, which increases the combustion flame temperature. The TB10 and diesel showed higher heat release rates, but TB10 showed higher NO_x than diesel. The higher NO_x is mainly due to higher amounts of fuel getting injected, increasing the oxygen inside the chamber (Graboski and McCormick, 1998). For instance, Zhu et al. (2013) observed a decrease in NO_x emissions with a decreased intake of oxygen concentration. Fig. 3 shows higher mass fractions are noticed for the TB10 compared to DE10. Moreover, the mass fractions are higher at 100% load compared to 25% load (Figs. 2 and 3). From the numerical analysis conducted by Doppalapudi and Azad (2024), NO emissions are directly correlated with the mass fractions inside the chamber. Their simulation results revealed that high NO concentrations were observed in the fuel mass fraction regions. Hence, higher NO concentrations are observed near the high fuel mass fractions at 100% load. After the fuel injection, the liquid fuel phase gets converted to the vapour phase, where the fuel will be distributed more extensively (Li et al., 2011; Doppalapudi et al., 2023a). However, with high loads, the time available for this phase change through fuel atomization and evaporation is less and causes rapid combustion (Palash et al., 2013). During the rapid combustion, higher flame fronts formed across the cylinder and caused higher NO_x emissions (Geng et al., 2017). Despite the higher oxygen availability in the TB10E10Eu10 blend, it showed lesser NO_x than diesel, TB10 and TB10E10 due to prolonged premixed combustion. As shown from the HRR graph (Fig. 13) at 100% load, TB10E10Eu10 peak HRR is noticed after TB10, which has increased the premixed combustion period. Hence, the prolonged premixed combustion has reduced the NO_x emissions. Azad et al. [51] presented that the NO_x generation rate mainly happens during the premixed combustion period. Similar results are also noted in the studies where high-oxygenated blended fuels showed reduced NO_x emissions (Mao et al., 2011; Nabi, 2010; Sendzikiene et al., 2006). Hence, factors like ID, mass fractions and premixed combustion play a significant role in NO_x emissions.

3.1.2. *Effect of ignition delay (ID) on NO_x emissions*

Fig. 4 presents the effect of ID on NO_x emissions with respect to

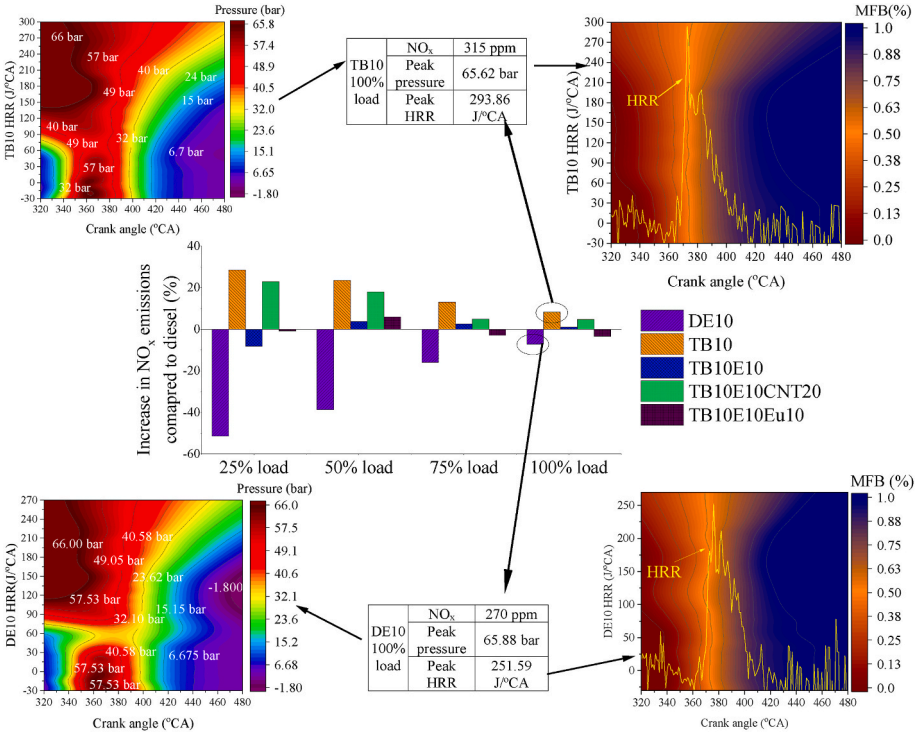

Fig. 3. Variation of NO_x emissions concerning loads and correlation of HRR and MFB combustion parameters at 100% load.

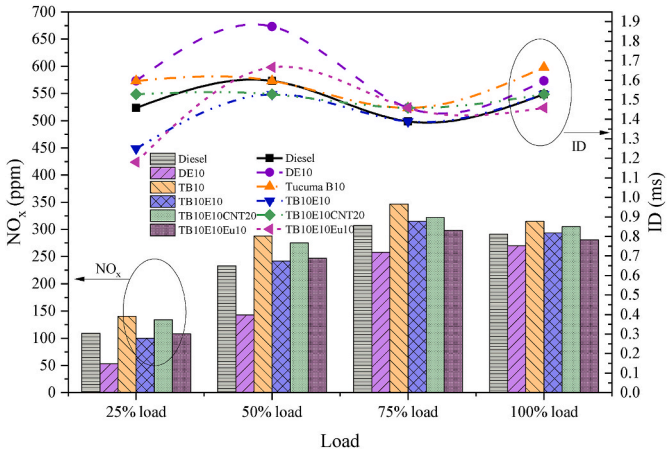

Fig. 4. Comparison of NO_x emissions and ID with respect to engine loads.

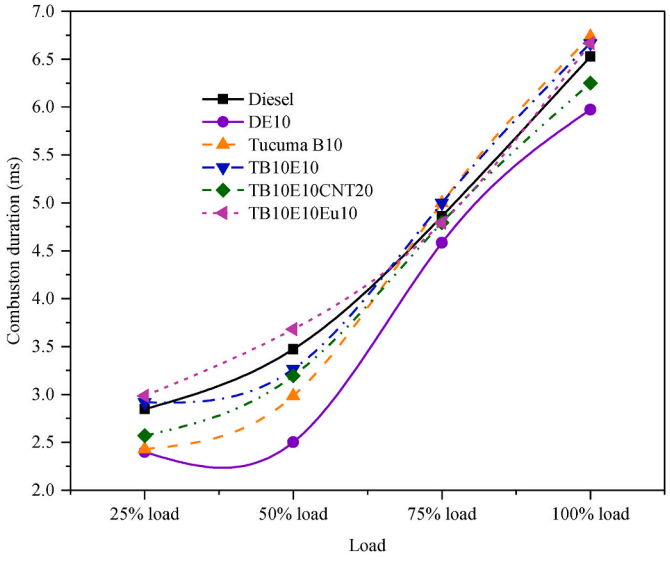

Fig. 5. Combustion duration for biodiesel blends with respect to loads.

Loads. At first, ID increased at 50% loads and then decreased at 75% loads, again decreasing at 100% load. A similar trend with the ID is also presented in the previous study conducted by Yoon et al. (2022). Higher ID is observed at 50% loads because the chamber conditions are inefficient for complete combustion. Factors like low compression temperatures, lower air-fuel turbulences, and decreased fuel evaporation rate have reduced the in-cylinder temperatures and increased the ID period (Mustayen et al., 2022). At lower loads, a longer ID is noted for DE10. Higher latent heat of vaporization of ethanol prolongs the ID by limiting the peak temperature formation inside the chamber and reducing the NO_x emissions. At the same time, as shown in Fig. 5, CD is lower for the DE10, and reduced CD revealed lower NO_x. From the review conducted by Doppalapudi et al. (2023b) stated that reduced NO_x is observed with fuels that showed longer ID and shorter CD. On the other hand, shorter ID and more extended CD are noted for the TB10E10Eu10, and NO_x was reduced at all loads. Besides, shorter ID is observed for the TB10E10CNT20 compared to TB10 and TB10E10, where the higher combustion temperatures and pressures build during the premixed stages and increase the NO_x emissions. For instance, Ooi et al. (2023) conducted engine tests by blending palm oil with multi-walled CNTs at varying speeds. The study reported that with the addition of CNTs, ID was reduced, and NO_x was increased by 21% with the addition of 25 ppm to the B20 blend. Solmaz et al. (2021) reported that MWCNTs conductivity is 2000 times greater than that of diesel, promoting faster fuel evaporation. Consequently, as the concentration of MWCNTs in the fuel blend rises, the mixture preparation improves by shortening the ID, leading to increased NO_x levels (Gharehghani and Pourrahmani, 2019). An increase in NO_x emission with the addition of MWCNTs to the biodiesel was also reported in Solmaz et al. (2023), Kocakulak et al. (2023) and Hosseinzadeh-Bandbafha et al. (2023). However, Elkelawy et al. (2023) revealed that the addition of CNTs has dramatically reduced NO_x emissions because of lower CD, which has reduced the residence time of the combustion.

3.1.3. *Influence of performance parameters on NO_x emissions*

Fig. 6 presents the relationship between performance characteristics and NO_x emissions with respect to engine load conditions. As shown in Fig. 6 (a), NO_x emissions increase with the increase in fuel-specific chemical exergy. For all the fuel blends, NO_x emissions increased with the increasing BMEP to 6 bar and started decreasing with the growing BMEP (Fig. 6 (b)). Lower NO_x for DE10 is due to the lower pressures developed at lower BMEP, which has reduced the HRR. Similar results were also reported in by Chen et al. [75] at 1000 rpm with varying BP. Fig. 6(c) depicts the relation between the BSFC and NO_x emissions, where the NO_x emissions are proportional to the specific fuel consumption. DE10 has shown less consumption at low loads; hence, lower ranges of NO_x are observed. Fig. 6(d) presents the relationship between EGT temperatures and NO_x emissions. As stated before, NO_x emissions are formed mainly because of the in-cylinder temperatures caused by rapid combustion. The study considered the EGT as the peak cylinder temperatures inside the chambers at the respective loads to correlate the relation between the EGT and NO_x emission. Both EGT and NO_x increase with increasing loads. TB10 showed higher EGT and higher NO_x at all loads, whereas diesel showed higher EGT at 75% of loads and less NO_x than TB10. This is mainly due to higher oxygen content in the combustion chamber with TB10 than diesel. On the other hand, TB10E10Eu10 has higher oxygen content among all the fuels; however, their NO_x emissions are lower. Here, the combustion rates, such as shorter ID and more extended CD, prolonged the premixed combustion and decreased the NO_x emissions.

3.1.4. *Tradeoff between CO and CO_2 emissions*

Fig. 7 demonstrates the percentage change in CO and CO_2 emissions compared to diesel at different load conditions. Ethanol blended fuels showed higher CO emissions at low load conditions; the emissions decreased with the increasing load. At 25% load, ethanol blended samples such as DE10, TB10E10, TB10E10CNT20, and TB10E10Eu10 have showed increased CO by 196%, 50.3%, 19.39%, and 55.15%, respectively, compared to diesel. TB10 showed reduced CO at all loads; however, at high loads, the CO emissions increased by 41%. The main reason is that the higher acid value of the Tucuma has caused higher CO emissions. Higher CO emissions with CNTs and Eucalyptus blends were noticed at 25% loads with the Tucuma-ethanol blends. The presence of CNTs in the fuel has increased the combustion rate and has reduced the CO emission at higher loads. At higher loads, increased CO_2 emissions are noted for all the fuels because at higher temperatures, CO emissions oxidized to form CO_2 (Binboğa, 2022). Diesel fuel emits higher CO emissions due to the absence of oxygen in its structure, but the addition of ethanol (35% oxygen content by weight) has shown an increase in CO emissions at 25% 50%, and 75% load conditions. This demonstrates the effect of heating value on the emissions. As discussed before, due to the lower heating value of the ethanol, at low loads, the combustion temperature is lower, hence the higher CO emissions. As a result, lower CO_2 emissions are noticed with the ethanol blends. Similar behaviour was also observed with the TB10E10Eu10, where higher CO emissions are noticed at lower loads and decreased with the increasing loads.

3.1.5. *Variation of HC emissions with varying loads*

Fig. 8 presents the variation of HC emissions for different biodiesel

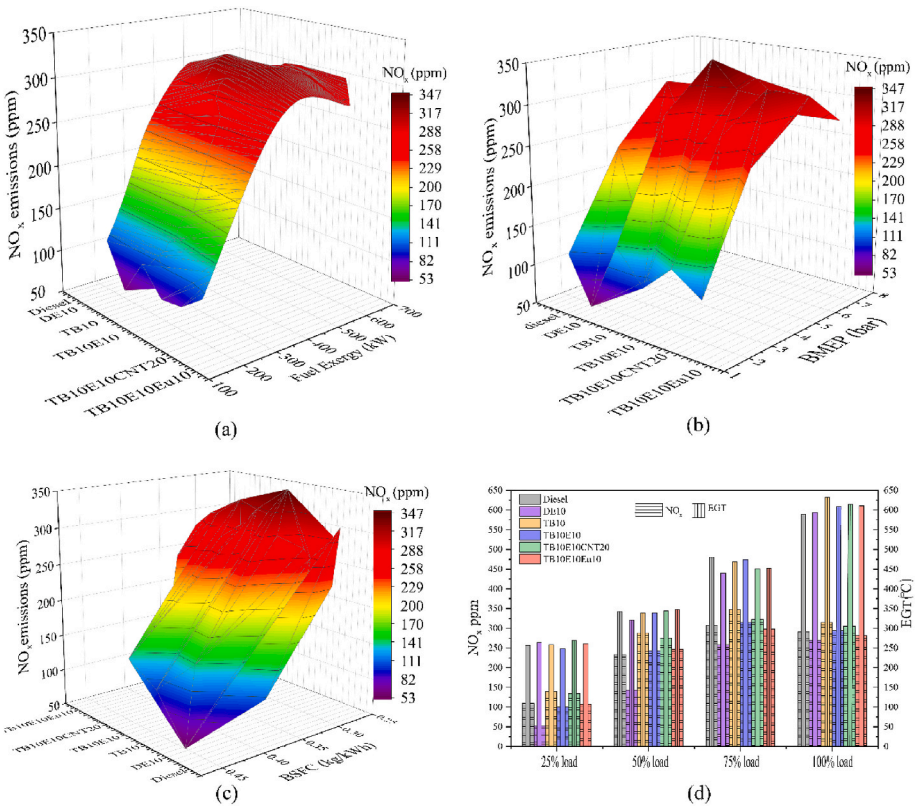

Fig. 6. Comparison of NO_x emissions with performance parameters; 5(a) NO_x vs Fuel exergy vs Load; 5(b) NO_x vs BMEP vs Load; 5(c) NO_x vs BSFC vs Load; 5(d) NO_x vs EGT vs Load.

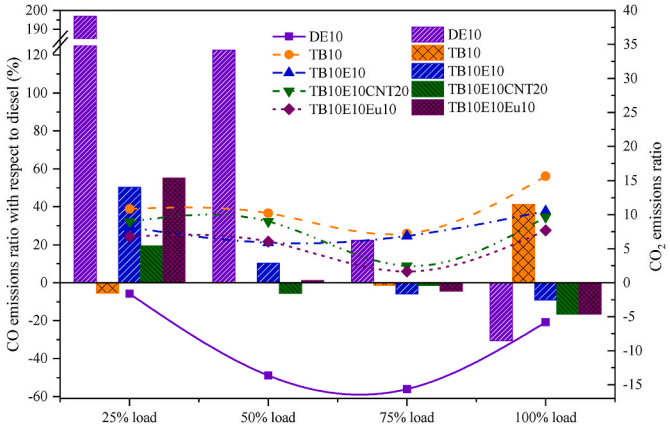

Fig. 7. Comparison of CO and CO_2 emissions with respect to load conditions.

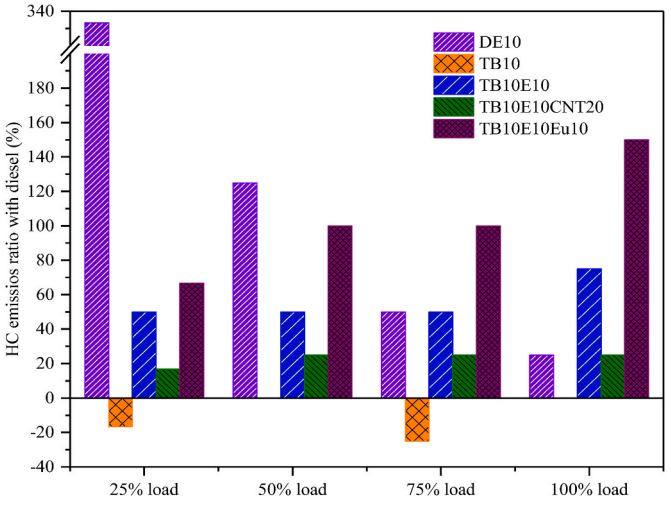

Fig. 8. Variation of HC emissions with respect to loads.

fuels compared to diesel fuel. Higher HC emissions are noticed with the DE10 blend at low loads, decreasing with the increasing load. Compared to diesel, HC emissions are increased for DE10 by 333%, 125%, 50% and 25.2% at 25% load, 50% load, 75% load and 100% load conditions. Mofijur et al. (2015) observed an approximately 500% increase in HC emissions with 15% ethanol blended fuel compared to the standard diesel. Similar behaviour is also noticed in the studies of Ferreira et al. [77] and Fang et al. (2013). A reverse trend is seen with the TB10E10Eu20, TB10E10 and TB10E10CNT20 blends, where the HC emissions increase with the increasing load conditions. TB10E10 showed a 50% increase in HC at 25%,50% and 75% load conditions; at 100% load, a 75.2% increase in HC emissions is noted compared to diesel. At higher loads, a 150% increase in HC emissions is noticed for the TB10E10Eu10 blend compared to diesel. The presence of lower active radicles in the blend and limited time availability for the combustion at higher loads have caused an increase in HC emissions. In the previous studies conducted by Rahman and Fattah (2023) and Gad et al. (2021), the addition of pure essential oils has reduced HC emissions compared to diesel. However, in this study, the increased emissions with pure essential oil blends are due to mixtures of turmeric, ethanol, eucalyptus, and diesel fuel. The fuel's higher density and lower calorific value have affected the hydrocarbons thermal breakdown, thereby increasing the HC emissions.

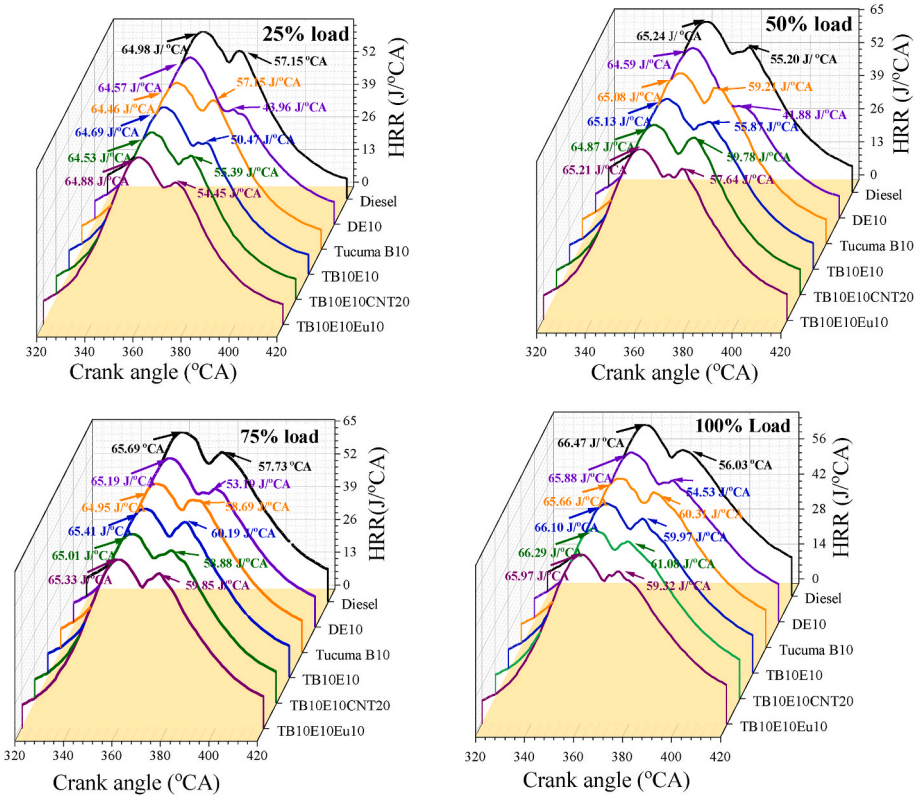

Fig. 9. Variation of in-cylinder pressures at different loads.

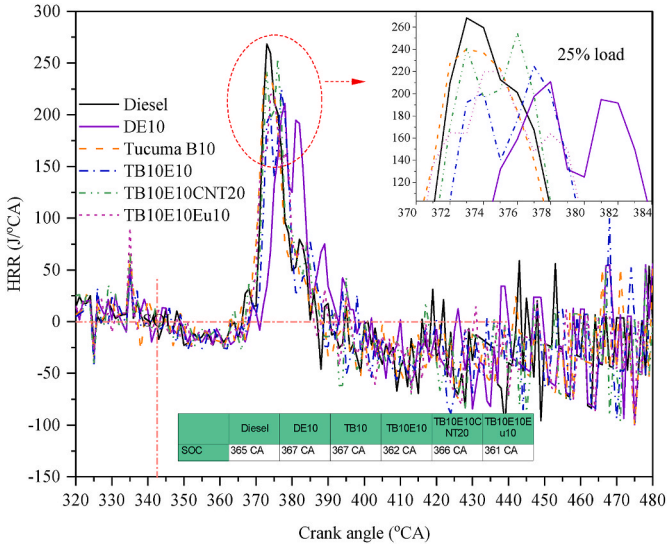

Fig. 10. Comparison of tested fuel blends HRR at 25% engine load condition.

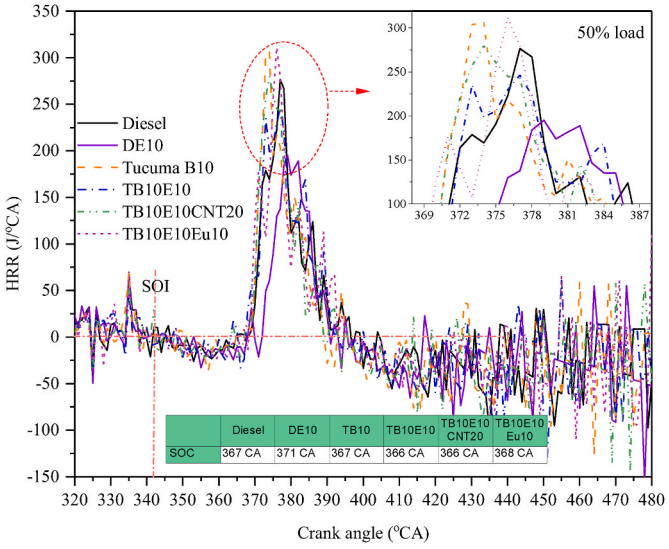

Fig. 11. Comparison of HRR at 50% for different fuel blends.

3.2. Combustion analysis

3.2.1. In-cylinder pressure analysis

Fig. 9 illustrates the variation of cylinder pressure for the tested fuels at 25% load, 50% load, 75% load and 100% load conditions. The figure shows that two peaks are noticed for the pressure curves, where the maximum peak is seen at 360 °CA (when the piston is at TDC), and the second peak is caught during the combustion stroke. Among all, DE10 showed lower peak pressures at 25% load, and DE10 showed higher pressures across the combustion stroke. As mentioned earlier, adding ethanol has reduced the in-cylinder pressures due to the vaporization cooling of ethanol. Similar results are also observed in studies Tsang et al. (2010) and Padala et al. (2013). At 50%, 75% and 100% test load conditions, DE10 showed lower pressure rates during the combustion stroke than all other fuels. At 25% load, DE10 and TB10 showed similar peak pressures of 57.15 bar and 57.45 bar, respectively. However, with the increasing loads, biodiesel blends such as TB10, TB10E10, TB10E10CNT20 and TB10E10Eu10 showed higher peak pressures compared to diesel and DE10. For instance, the second peak pressures at 50% load are in the order of TB10E10CNT20 (59.78 bar), TB10(59.26 bar), TB10E10Eu10 (57.64 bar), TB10E10 (56 bar), diesel (55.20 bar) and DE10 (42.14 bar), respectively.

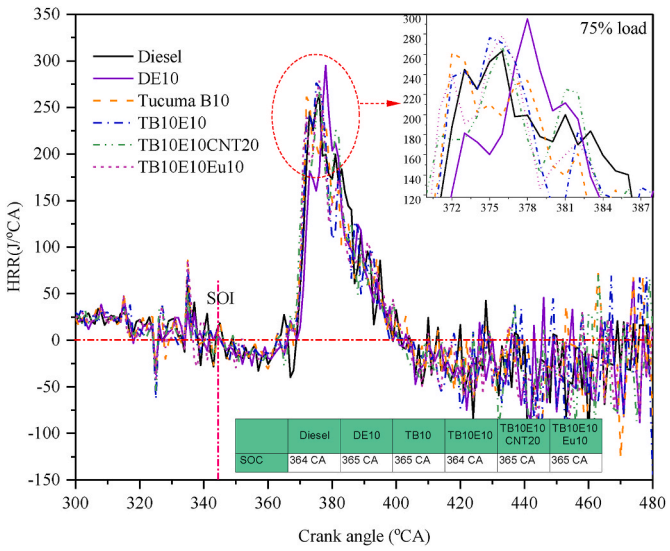

Fig. 12. Comparison of HRR for tested fuel blends at 75% engine load.

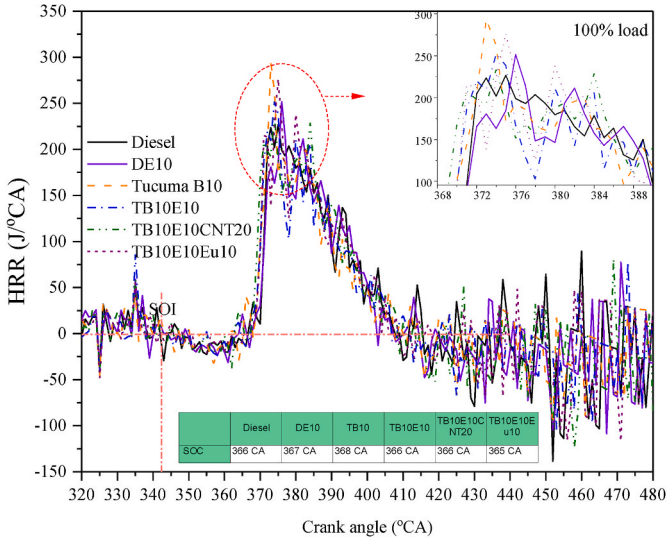

Fig. 13. Comparison of HRR at 100% load for different fuel blends.

3.2.2. In-cylinder heat release rate (HRR) analysis

Figs. 10–13 illustrate the heat release rates for diesel and biodiesel in different blends. As depicted in Figure *10*, a higher heat release rate is noticed for the diesel fuel 268.5 J at 373°CA. At lower loads, the in-cylinder combustion temperatures are low, which makes it difficult for the biodiesel blends to get combustible. Following diesel, TB10E10CNT10 showed peak HRR at 254.7 J at 376°CA. The presence of CNTs has increased the combustion rates; however, the mixture showed a longer ID due to the ethanol blending. Rajpoot et al. (2023) observed reduced ID with the addition of CNTs to soybean biodiesel compared to diesel. This is due to the higher thermal conductivity of CNT nanoparticles, which has enhanced the combustion process. Both DE10 (203 J/°CA) and TB10E10 (200 J/°CA) have shown reduced peak HRR and longer ID compared to all the tested blends. As shown in Fig. 11, higher heat release rates are noticed for the TB10 (306.5J at 373 °CA) and TB10E10Eu10 (311 J at 376 °CA) compared to diesel (279 J at 377 °CA) and other blends at 50% load conditions. Early start of combustion (SOC) is noticed for TB10 and TB10E10Eu10 compared to diesel. This advancement in SOC is mainly due to higher oxygen content, fewer aromatics, and a higher cetane number in the biodiesel blends (Rodríguez et al., 2011; Kuti et al., 2013). Similar results were also reported by Öztürk and Can (2022) at low and partial load conditions, where advancements in ID is noticed for biodiesel blends compared to diesel.

DE10 showed higher HRR rates at higher loads as the combustion improved for ethanol blends at higher loads. At 75% load (Fig. 12), peak HRR is noticed for DE10 295.2 J at 378 °CA with a longer ignition delay. Lower cetane number of the ethanol prolonged the ID period. Due to the higher temperature conditions at high loads, the prolonged ID provides time for the premixed combustion and increases the HRR. Similar results are also reported by Zhu et al. (2011) and Kumar et al. (2006).

3.3. Fuel exergy, energy and performance analysis

3.3.1. Comparison of BTE and fuel exergy with varying load

Fig. 14 illustrates the relation between the fuel exergy and the BTE at varying loads. Fig. 14 depicts that BTE increases with the increasing loads till the 75% load condition, and a decrease in BTE is observed at the 100% load condition. On the other hand, fuel exergy increased with the increasing loads. At 100% load, higher fuel exergy is noted for TB10E10 (601.56 kW), followed by diesel (594.13 kW), TB10E10Eu10 (593.9 kW), TB10 (591.8 kW), TB10E10CNT20 (585.7 kW) and DE10 (538.53 kW), respectively. As shown in Fig. 14, at one specific load condition, BTE and fuel exergy are inversely proportional. For instance, at 25% load, TB10E10Eu10 showed a lower exergy of 180.33 kW compared to all other fuels, but at the same load, the blend showed a higher BTE of 23.93% than all other blends, including diesel. Similarly, DE10 showed a lower fuel exergy (538.53 kW) rate at 100% load, whereas higher BTE is noted for DE10 (32.24%) than other fuels. TB10 showed better BTE than others, but at 100% load condition, TB10 showed a 2.7% decrease in BTE compared to diesel. At 75% load condition, DE10, TB10, TB10E10 and TB10E10CNT20 showed an increase in BTE by 5.3%, 4.75%, 0.5% and 2.71%, respectively, compared to diesel. At 25% load, TB10E10Eu10 showed a 9% increase in BTE compared to diesel, whereas, at 100% load, the same blend showed a 6% decrease in BTE compared to diesel. The reduced BTE at higher loads is due to the lower calorific value and reduced time availability for better combustion.

3.3.2. Comparison of BSFC and fuel energy with varying load

Fig. 15 compares fuel energy and specific fuel consumption at different load conditions for the tested fuel blends. Among all the blends, diesel has higher fuel energy; hence, the lesser BSFC values are noted in all load conditions. DE10 blend has lower specific fuel energy, but the higher BSFC is noted for DE10 only at 25% load. Next to diesel, at 75% and 100% load, DE10 showed less BSFC than others. This is because higher activation temperatures are required for the combustion of

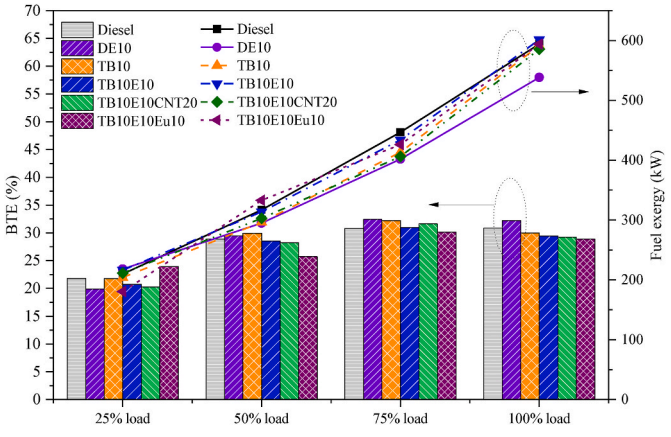

Fig. 14. Comparison of BTE and specific fuel exergy with respect to loads.

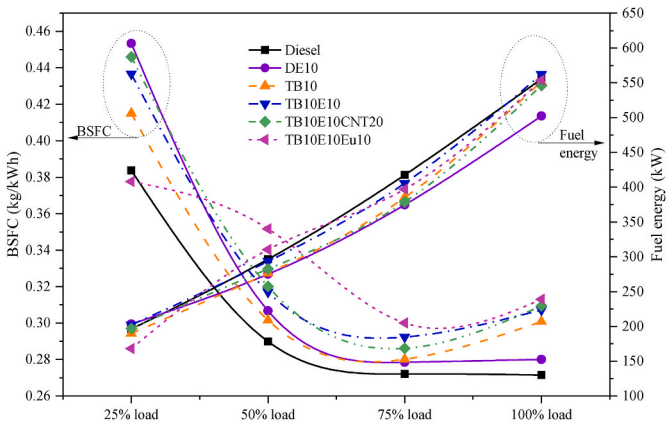

Fig. 15. Comparison of BSFC and fuel energy with varying loads.

ethanol blends. Hence, as per the HRR graphs Figs. 10–13, ethanol composition in fuel has shown higher cylinder pressures and heat release rates at higher loads. A similar pattern is also reported in the studies of Barabás and Todoruţ (2011) and Barabas et al. (2010). Higher BSFC is noted for ethanol blended fuel than the TB10 operation. TB10E10Eu10 has shown higher BSFC than all other fuel blends at varying load conditions. This adverse effect is mainly due to its lower calorific value than others, as presented in Table 1. The addition of nanoparticles to the TB10E10 blend has shown reduced BSFC at higher loads compared to the TB10E10 blend alone. For instance, at 75% load, TB10E10CNT20 showed a 21.5% reduction in BSFC compared to TB10E10; however, the same blend showed a 2.16% increase in BSFC compared to TB10. On the other hand, higher viscosity is noted for the TB10, TB10E10 and TB10E10CNT20 compared to diesel. This is mainly due to the higher viscosity of the blends. During the injection, the higher kinematic viscosity of the fuel affects the fuel atomization and evaporation process, resulting in poor combustion. Similar results are also noticed in studies by Chammoun et al. (2013), Shehata and Razek (2011), and Rajan and Senthilkumar (2009).

4. Conclusions and recommendations

This study specifically aimed at reducing NO_x emissions from diesel engines using Tucuma biodiesel. Fuel modifications, such as blending Tucuma biodiesel with ethanol, carbon nanotubes (CNTs), and eucalyptus oil, were carried out on a 4-cylinder tractor engine under different load conditions, and the conclusions are as follows.

1) Ethanol blends showed less CO at low loads due to low-temperature formation, that caused lower CO oxidation. Further addition CNTs enhanced the combustion rates and lowered CO emissions compared to ethanol and biodiesel blends. Higher HC is noticed for ethanol-blended fuels at low loads and was decreased with increasing loads. On the other hand, TB10E10Eu10 showed increased HC emissions with the increasing loads.
2) Higher NO_x is observed for TB10 (315 ppm), followed by TB10E10CNT20 (305 ppm), TB10E10 (294 ppm), diesel (291 ppm), TB10E10Eu10 (281 ppm) and DE10 (270 ppm). A shorter ID and longer CD were noted for the TB10E10Eu10 and showed reduced NO_x at all loads. DE10 has shown less fuel consumption at low loads and lower NO_x ranges.
3) Ethanol blended fuels have shown less effect on combustion at low loads, but higher HRR rates are observed at high loads. Longer ID is seen with ethanol blend but with the addition CNTs to the blend has reduced the ID period. Diesel has shown peak pressure rates and HRR at low loads, but at high loads, TB10 has shown peak pressure rates and high HRR. At 75% loads, TB10E10 showed increased pressure rates compared to all the blends.
4) At 75% load conditions, DE10, TB10, TB10E10, and TB10E10CNT20 exhibit higher BTE by 5.4%, 4.75%, 0.6%, and 2.71%, respectively, compared to diesel. Compared to all the blends, TB10E10Eu10 showed higher BSFC except for 25% load conditions due to poor calorific value.

The study recommends working on TB10E10 and TB10E10CNT20, as they have shown reduced NO_x and CO emissions compared to the biodiesel blend (TB10). Moreover, injection advancement studies are much needed as the ethanol-blended fuel showed longer ID with greater reductions in NO_x emissions.

CRediT authorship contribution statement

Arun Teja Doppalapudi: Writing – original draft, Validation, Software, Methodology, Investigation, Formal analysis, Data curation. **Abul Kalam Azad:** Writing – review & editing, Validation, Supervision, Resources, Methodology, Formal analysis, Conceptualization. **Mohammad Masud Kamal Khan:** Writing – review & editing, Supervision.

Declaration of competing interest

The authors declare that they have no known competing financial interests or personal relationships that could have appeared to influence the work reported in this paper.

Data availability

Data will be made available on request.

References

Agarwal, A.K., 2007. Biofuels (alcohols and biodiesel) applications as fuels for internal combustion engines. Prog. Energy Combust. Sci. 33, 233–271.
Alptekin, E., 2017. Emission, injection and combustion characteristics of biodiesel and oxygenated fuel blends in a common rail diesel engine. Energy 119, 44–52.
Alptekin, E., Canakci, M., Ozsezen, A.N., Turkcan, A., Sanli, H., 2015. Using waste animal fat based biodiesels–bioethanol–diesel fuel blends in a DI diesel engine. Fuel 157, 245–254.
Annamalai, M., Dhinesh, B., Nanthagopal, K., Sivaramakrishnan, P., Lalvani, J.I.J., Parthasarathy, M., Annamalai, K., 2016. An assessment on performance, combustion and emission behavior of a diesel engine powered by ceria nanoparticle blended emulsified biofuel. Energy Convers. Manag. 123, 372–380.
Ashok, B., Nanthagopal, K., Saravanan, B., Azad, K., Patel, D., Sudarshan, B., Aaditya Ramasamy, R., 2019. Study on isobutanol and Calophyllum inophyllum biodiesel as a partial replacement in CI engine applications. Fuel 235, 984–994.
Atabani, A.E., Silitonga, A.S., Badruddin, I.A., Mahlia, T.M.I., Masjuki, H.H., Mekhilef, S., 2012. A comprehensive review on biodiesel as an alternative energy resource and its characteristics. Renew. Sustain. Energy Rev. 16, 2070–2093.
Atadashi, I., Aroua, M.K., Aziz, A.A., 2010a. High quality biodiesel and its diesel engine application: a review. Renew. Sustain. Energy Rev. 14, 1999–2008.
Atadashi, I.M., Aroua, M.K., Aziz, A.A., 2010b. High quality biodiesel and its diesel engine application: a review. Renew. Sustain. Energy Rev. 14, 1999–2008.
Azad, A.K., 2017. Biodiesel from Mandarin Seed Oil: A Surprising Source of Alternative Fuel, 10. Energies [Online].
Azad, A.K., Doppalapudi, A.T., Khan, M.M.K., Hassan, N.M.S., Gudimetla, P., 2023a. A landscape review on biodiesel combustion strategies to reduce emission. Energy Rep. 9, 4413–4436.
Azad, A.K., Halder, P., Wu, Q., Rasul, M.G., Hassan, N.M.S., Karthickeyan, V., 2023b. Experimental investigation of ternary biodiesel blends combustion in a diesel engine to reduce emissions. Energy Convers. Manag. X 20, 100499.
Azad, A.K., Jadeja, A.C., Doppalapudi, A.T., Hassan, N.M., Nabi, M.N., Rauniyar, R., 2024. Design and Simulation of the Biodiesel Process Plant for Sustainable Fuel Production, 16. *Sustainability* [Online].
Azad, A.K., Rasul, M.G., Khan, M.M.K., Sharma, S.C., Bhuiya, M.M.K., 2016. Recent development of biodiesel combustion strategies and modelling for compression ignition engines. Renew. Sustain. Energy Rev. 56, 1068–1086.
Balat, M., Balat, H., 2010. Progress in biodiesel processing. Appl. Energy 87, 1815–1835.
Banapurmath, N., Sankaran, R., Tumbal, A., Narasimhalu, N., Hunshyal, A., Ayachit, N., 2014. Experimental investigation on direct inj. diesel engine fuelled with graphene, silver and multiwalled carbon nanotubes-biodiesel blended fuels. Int. J. Adv. Eng. Technol. 3, 129–138.
Barabas, I., Todoruţ, A., Băldean, D., 2010. Performance and emission characteristics of an CI engine fueled with diesel–biodiesel–bioethanol blends. Fuel 89, 3827–3832.
Barabás, I., Todoruţ, I.-A., 2011. Utilization of biodiesel-diesel-ethanol blends in CI engine. Biodiesel-quality, emissions and by-products, InTech 215–234.

Basha, J.S., Anand, R., 2011. An experimental investigation in a diesel engine using carbon nanotubes blended water–diesel emulsion fuel. Proc. Inst. Mech. Eng. A J. Power Energy 225, 279–288.
Basha, J.S., Anand, R., 2014. Performance, emission and combustion characteristics of a diesel engine using Carbon Nanotubes blended Jatropha Methyl Ester Emulsions. Alex. Eng. J. 53, 259–273.
Bhuiya, M.M.K., Rasul, M.G., Khan, M.M.K., Ashwath, N., Azad, A.K., Mofijur, M., 2015. Optimisation of oil extraction process from Australian native beauty leaf seed (Calophyllum inophyllum). Energy Proc. 75, 56–61.
Binboğa, F., 2022. VECTO Review: Reducing CO2 Emissions from Heavy Duty Vehicles.
Boningari, T., Smirniotis, P.G., 2016. Impact of nitrogen oxides on the environment and human health: Mn-based materials for the NOx abatement. Current Opinion in Chemical Engineering 13, 133–141.
Butkus, A., Pukalskas, S., Bogdanovičius, Z., 2007. The influence of turpentine additive on the ecological parameters of diesel engines. Transport 22, 80–82.
Chammoun, N., Geller, D.P., Das, K., 2013. Fuel properties, performance testing and economic feasibility of Raphanus sativus (oilseed radish) biodiesel. Ind. Crop. Prod. 45, 155–159.
Datta, A., Mandal, B.K., 2017. Engine performance, combustion and emission characteristics of a compression ignition engine operating on different biodiesel-alcohol blends. Energy 125, 470–483.
Demirbas, A., 2007. Importance of biodiesel as transportation fuel. Energy Pol. 35, 4661–4670.
Devan, P.K., Mahalakshmi, N.V., 2009. Performance, emission and combustion characteristics of poon oil and its diesel blends in a DI diesel engine. Fuel 88, 861–867.
Doppalapudi, A.T., Azad, A.K., 2024. Advanced numerical analysis of in-cylinder combustion and NOx formation using different chamber geometries. Fire [Online] 7.
Doppalapudi, A.T., Azad, A.K., Khan, M.M., 2023a. Analysis of improved in-cylinder combustion characteristics with chamber modifications of the diesel engine. Energies 16 [Online].
Doppalapudi, A.T., Azad, A.K., Khan, M.M.K., 2021. Combustion chamber modifications to improve diesel engine performance and reduce emissions: a review. Renew. Sustain. Energy Rev. 152, 111683.
Doppalapudi, A.T., Azad, A.K., Khan, M.M.K., 2023b. Advanced strategies to reduce harmful nitrogen-oxide emissions from biodiesel fueled engine. Renew. Sustain. Energy Rev. 174, 113123.
El-Seesy, A.I., Abdel-Rahman, A.K., Bady, M., Ookawara, S., 2017. Performance, combustion, and emission characteristics of a diesel engine fueled by biodiesel-diesel mixtures with multi-walled carbon nanotubes additives. Energy Convers. Manag. 135, 373–393.
Elkelawy, M., Bastawissi, H.A.-E., Esmaeil, K.K., Radwan, A.M., Panchal, H., Sadasivuni, K.K., Ponnamma, D., Walvekar, R., 2019. Experimental studies on the biodiesel production parameters optimization of sunflower and soybean oil mixture and DI engine combustion, performance, and emission analysis fueled with diesel/biodiesel blends. Fuel 255, 115791.
Elkelawy, M., El Shenawy, E.S.A., Bastawissi, H.A., Shams, M.M., 2023. Impact of carbon nanotubes and graphene oxide nanomaterials on the performance and emissions of diesel engine fueled with diesel/biodiesel blend. Processes 11 [Online].
Emiroğlu, A.O., Şen, M., 2018. Combustion, performance and exhaust emission characterizations of a diesel engine operating with a ternary blend (alcohol-biodiesel-diesel fuel). Appl. Therm. Eng. 133, 371–380.
Fang, Q., Fang, J., Zhuang, J., Huang, Z., 2013. Effects of ethanol–diesel–biodiesel blends on combustion and emissions in premixed low temperature combustion. Appl. Therm. Eng. 54, 541–548.
Ferreira, V.P., Martins, J., Torres, E.A., Pepe, I.M., De Souza, J.M.R., 2013. Performance and emissions analysis of additional ethanol injection on a diesel engine powered with A blend of diesel-biodiesel. Energy for Sustainable Development 17, 649–657.
Gad, M.S., He, Z., El-Shafay, A.S., El-Seesy, A.I., 2021. Combustion characteristics of a diesel engine running with Mandarin essential oil -diesel mixtures and propanol additive under different exhaust gas recirculation: experimental investigation and numerical simulation. Case Stud. Therm. Eng. 26, 101100.
Geng, P., Cao, E., Tan, Q., Wei, L., 2017. Effects of alternative fuels on the combustion characteristics and emission products from diesel engines: a review. Renew. Sustain. Energy Rev. 71, 523–534.
Gerpen, J.V., 2005. Biodiesel processing and production. Fuel Process. Technol. 86, 1097–1107.
Gharehghani, A., Asiaei, S., Khalife, E., Najafi, B., Tabatabaei, M., 2019. Simultaneous reduction of CO and NOx emissions as well as fuel consumption by using water and nano particles in Diesel–Biodiesel blend. J. Clean. Prod. 210, 1164–1170.
Gharehghani, A., Mirsalim, M., Hosseini, R., 2017. Effects of waste fish oil biodiesel on diesel engine combustion characteristics and emission. Renew. Energy 101, 930–936.
Gharehghani, A., Pourrahmani, H., 2019. Performance evaluation of diesel engines (PEDE) for a diesel-biodiesel fueled CI engine using nano-particles additive. Energy Convers. Manag. 198, 111921.
Graboski, M.S., Mccormick, R.L., 1998. Combustion of fat and vegetable oil derived fuels in diesel engines. Prog. Energy Combust. Sci. 24, 125–164.
Guarieiro, L.L.N., De Souza, A.F., Torres, E.A., De Andrade, J.B., 2009. Emission profile of 18 carbonyl compounds, CO, CO2, and NOx emitted by a diesel engine fuelled with diesel and ternary blends containing diesel, ethanol and biodiesel or vegetable oils. Atmos. Environ. 43, 2754–2761.
Guo, Y., Zhu, L., Wang, X., Qiu, X., Qian, W., Wang, L., 2022. Assessing environmental impact of NOX and SO2 emissions in textiles production with chemical footprint. Sci. Total Environ. 831, 154961.
Halder, P., Azad, K., Shah, S., Sarker, E., 2019. 8 - prospects and technological advancement of cellulosic bioethanol ecofuel production. In: AZAD, K. (Ed.), Advances in Eco-Fuels for a Sustainable Environment. Woodhead Publishing.
Hao, D., Liu, Y., Gao, S., Arandiyan, H., Bai, X., Kong, Q., Wei, W., Shen, P.K., Ni, B.-J., 2021. Emerging artificial nitrogen cycle processes through novel electrochemical and photochemical synthesis. Mater. Today 46, 212–233.
He, B.-Q., Shuai, S.-J., Wang, J.-X., He, H., 2003. The effect of ethanol blended diesel fuels on emissions from a diesel engine. Atmos. Environ. 37, 4965–4971.
Heydari-Maleney, K., Taghizadeh-Alisaraei, A., Ghobadian, B., Abbaszadeh-Mayvan, A., 2017. Analyzing and evaluation of carbon nanotubes additives to diesohol-B2 fuels on performance and emission of diesel engines. Fuel 196, 110–123.
Hosseini, S.H., Taghizadeh-Alisaraei, A., Ghobadian, B., Abbaszadeh-Mayvan, A., 2017. Performance and emission characteristics of a CI engine fuelled with carbon nanotubes and diesel-biodiesel blends. Renew. Energy 111, 201–213.
Hosseinzadeh-Bandbafha, H., Kazemi Shariat Panahi, H., Dehhaghi, M., Orooji, Y., Shahbeik, H., Mahian, O., Karimi-Maleh, H., Kalam, M.A., Salehi Jouzani, G., Mei, C., Nizami, A.-S., Guillemin, G.G., Gupta, V.K., Lam, S.S., Yang, Y., Peng, W., Pan, J., Kim, K.-H., Aghbashlo, M., Tabatabaei, M., 2023. Applications of nanotechnology in biodiesel combustion and post-combustion stages. Renew. Sustain. Energy Rev. 182, 113414.
Hulwan, D.B., Joshi, S.V., 2011. Performance, emission and combustion characteristic of a multicylinder DI diesel engine running on diesel–ethanol–biodiesel blends of high ethanol content. Appl. Energy 88, 5042–5055.
Jena, P.C., Raheman, H., Kumar, G.P., Machavaram, R., 2010. Biodiesel production from mixture of mahua and simarouba oils with high free fatty acids. Biomass Bioenergy 34, 1108–1116.
Khoobbakht, G., Najafi, G., Karimi, M., Akram, A., 2016. Optimization of operating factors and blended levels of diesel, biodiesel and ethanol fuels to minimize exhaust emissions of diesel engine using response surface methodology. Appl. Therm. Eng. 99, 1006–1017.
Kishore, K., Kurien, C., Mittal, M., 2024. Experimental and numerical analysis of engine characteristics of an ammonia-substituted dual-fuel CRDI diesel engine. Fuel 366, 131354.
Knothe, G., 2010. Biodiesel and renewable diesel: a comparison. Prog. Energy Combust. Sci. 36, 364–373.
Kocakulak, T., Arslan, T.A., Şahin, F., Solmaz, H., Ardebili, S.M.S., Calam, A., 2023. Determination of optimum operating parameters of MWCNT-doped ethanol fueled HCCI engine for emission reduction. Sci. Total Environ. 895, 165196.
Köse, S., Babagiray, M., Kocakulak, T., 2021. Response surface method based optimization of the viscosity of waste cooking oil biodiesel. Eng Perspect 1, 30–37.
Krishnan, M.G., Rajkumar, S., 2022. Effects of dual fuel combustion on performance, emission and energy-exergy characteristics of diesel engine fuelled with diesel-isobutanol and biodiesel-isobutanol. Energy 252, 124022.
Kumar, M.S., Kerihuel, A., Bellettre, J., Tazerout, M., 2006. Ethanol animal fat emulsions as a diesel engine fuel – Part 2: engine test analysis. Fuel 85, 2646–2652.
Kuti, O.A., Zhu, J., Nishida, K., Wang, X., Huang, Z., 2013. Characterization of spray and combustion processes of biodiesel fuel injected by diesel engine common rail system. Fuel 104, 838–846.
Li, T., Nishida, K., Hiroyasu, H., 2011. Droplet size distribution and evaporation characteristics of fuel spray by a swirl type atomizer. Fuel 90, 2367–2376.
Li, Z., Hu, Y., Chen, L., Wang, L., Fu, D., Ma, H., Fan, L., An, C., Liu, A., 2018. Emission factors of NOx, SO2, and PM for bathing, heating, power generation, coking, and cement industries in Shanxi, China: based on field measurement. Aerosol Air Qual. Res. 18, 3115–3127.
Ma, D., Zhang, S., He, X., Ding, X., Li, W., Liu, P., 2024. Combustion stability and NOx emission characteristics of three combustion modes of pulverized coal boilers under low or ultra-low loads. Appl. Energy 353, 121998.
Manimaran, R., Mohanraj, T., Ashwin, R., 2023. Green synthesized nano-additive dosed biodiesel-diesel-water emulsion blends for CI engine application: performance, combustion, emission, and exergy analysis. J. Clean. Prod. 413, 137497.
Mao, G., Wang, Z., Hu, P., Ni, P., Wang, X., Gu, S.-Q., 2011. Experimental research on the flame temperature of biodiesel fuel combustion in open-air conditions. In: 2011 International Conference on Electric Information and Control Engineering, pp. 2171–2174.
Mendera, K.Z., Spyra, A., Smereka, M., 2002. Mass fraction burned analysis. Journal of KONES Internal Combustion Engines 3, 193–201.
Mirhashemi, F.S., Sadrnia, H., 2020. NOX emissions of compression ignition engines fueled with various biodiesel blends: a review. J. Energy Inst. 93, 129–151.
Mofijur, M., Rasul, M., Hyde, J., 2015. Recent developments on internal combustion engine performance and emissions fuelled with biodiesel-diesel-ethanol blends. Procedia Eng. 105, 658–664.
Mosarof, M., Kalam, M., Masjuki, H., Alabdulkarem, A., Ashraful, A., Arslan, A., Rashedul, H., Monirul, I., 2016. Optimization of performance, emission, friction and wear characteristics of palm and Calophyllum inophyllum biodiesel blends. Energy Convers. Manag. 118, 119–134.
Murugesan, P., Elumalai, P.V., Balasubramanian, D., Padmanabhan, S., Murugunachippan, N., Afzal, A., Sharma, P., Kiran, K., Femilda Josephin, J.S., Varuvel, E.G., Tuan Le, T., Truong, T.H., 2023. Exploration of low heat rejection engine characteristics powered with carbon nanotubes-added waste plastic pyrolysis oil. Process Saf. Environ. Protect. 176, 1101–1119.
Mustayen, A.G.M.B., Wang, X., Rasul, M.G., Hamilton, J.M., Negnevitsky, M., 2022. Thermodynamic analysis of diesel engine ignition delay under low load conditions. Energy Rep. 8, 495–501.
Nabi, M.N., 2010. Theoretical investigation of engine thermal efficiency, adiabatic flame temperature, NOx emission and combustion-related parameters for different oxygenated fuels. Appl. Therm. Eng. 30, 839–844.

Nabi, M.N., Hustad, J.E., Arefin, M.A., 2020. The influence of Fischer–Tropsch-biodiesel–diesel blends on energy and exergy parameters in a six-cylinder turbocharged diesel engine. Energy Rep. 6, 832–840.
Nabi, M.N., Rasul, M., Anwar, M., Mullins, B., 2019a. Energy, exergy, performance, emission and combustion characteristics of diesel engine using new series of non-edible biodiesels. Renew. Energy 140, 647–657.
Nabi, M.N., Rasul, M.G., Anwar, M., Mullins, B.J., 2019b. Energy, exergy, performance, emission and combustion characteristics of diesel engine using new series of non-edible biodiesels. Renew. Energy 140, 647–657.
Najafi, G., Shadidi, B., 2024. The influence of single and multi-carbon nanotubes as additives in diesel-biodiesel fuel blends on diesel engine combustion characteristics, performance, and emissions. Biofuels 15, 177–190.
Odibi, C., Babaie, M., Zare, A., Nabi, M.N., Bodisco, T.A., Brown, R.J., 2019. Exergy analysis of a diesel engine with waste cooking biodiesel and triacetin. Energy Convers. Manag. 198, 111912.
Ooi, J.B., Kau, C.C., Manoharan, D.N., Wang, X., Tran, M.-V., Hung, Y.M., 2023. Effects of multi-walled carbon nanotubes on the combustion, performance, and emission characteristics of a single-cylinder diesel engine fueled with palm-oil biodiesel-diesel blend. Energy 281, 128350.
Öztürk, E., Can, Ö., 2022. Effects of EGR, injection retardation and ethanol addition on combustion, performance and emissions of a DI diesel engine fueled with canola biodiesel/diesel fuel blend. Energy 244, 123129.
Padala, S., Woo, C., Kook, S., Hawkes, E.R., 2013. Ethanol utilisation in a diesel engine using dual-fuelling technology. Fuel 109, 597–607.
Palash, S.M., Kalam, M.A., Masjuki, H.H., Masum, B.M., Rizwanul Fattah, I.M., Mofijur, M., 2013. Impacts of biodiesel combustion on NOx emissions and their reduction approaches. Renew. Sustain. Energy Rev. 23, 473–490.
Paul, A., Panua, R., Debroy, D., 2017. An experimental study of combustion, performance, exergy and emission characteristics of a CI engine fueled by Diesel-ethanol-biodiesel blends. Energy 141, 839–852.
Paul, A., Panua, R., Debroy, D., Kumar Bose, P., 2016. A performance-emission tradeoff study of a CI engine fueled by compressed natural gas (CNG)/diesel–ethanol-PPME blend combination. Environ. Prog. Sustain. Energy 35, 517–530.
Pedrozo, V.B., May, I., Dalla Nora, M., Cairns, A., Zhao, H., 2016. Experimental analysis of ethanol dual-fuel combustion in a heavy-duty diesel engine: an optimisation at low load. Appl. Energy 165, 166–182.
Purushothaman, K., Nagarajan, G., 2009. Experimental investigation on a CI engine using orange oil and orange oil with DEE. Fuel 88, 1732–1740.
Rahman, M.M., Rasul, M.G., Hassan, N.M.S., Azad, A.K., Uddin, M.N., 2017. Effect of small proportion of butanol additive on the performance, emission, and combustion of Australian native first- and second-generation biodiesel in a diesel engine. Environ. Sci. Pollut. Control Ser. 24, 22402–22413.
Rahman, S.M.A., Fattah, I.M.R., 2023. Evaluation of a compression ignition engine performance and emission characteristics using diesel-essential oil blends of high orange oil content. Aust. J. Mech. Eng. 21, 725–732.
Rahman, S.M.A., Nabi, M.N., Van, T.C., Suara, K., Jafari, M., Dowell, A., Islam, M.A., Marchese, A.J., Tryner, J., Hossain, M.F., Rainey, T.J., Ristovski, Z.D., Brown, R.J., 2018. Performance and combustion characteristics analysis of multi-cylinder CI engine using essential oil blends. Energies 11 [Online].
Rahman, S.M.A., Van, T.C., Hossain, F.M., Jafari, M., Dowell, A., Islam, M.A., Nabi, M.N., Marchese, A.J., Tryner, J., Rainey, T., Ristovski, Z.D., Brown, R.J., 2019. Fuel properties and emission characteristics of essential oil blends in a compression ignition engine. Fuel 238, 440–453.
Rajak, U., Nashine, P., Nath Verma, T., 2020. Numerical study on emission characteristics of a diesel engine fuelled with diesel-spirulina microalgae-ethanol blends at various operating conditions. Fuel 262, 116519.
Rajan, K., Senthilkumar, K., 2009. Effect of exhaust gas recirculation (EGR) on the performance and emission characteristics of diesel engine with sunflower oil methyl ester. Jordan Journal of Mechanical and Industrial Engineering 3, 306–311.
Rajpoot, A.S., Saini, G., Chelladurai, H.M., Shukla, A.K., Choudhary, T., 2023. Comparative combustion, emission, and performance analysis of a diesel engine using carbon nanotube (CNT) blended with three different generations of biodiesel. Environ. Sci. Pollut. Control Ser. 30, 125328–125346.
Rodríguez, R.P., Sierens, R., Verhelst, S., 2011. Ignition delay in a palm oil and rapeseed oil biodiesel fuelled engine and predictive correlations for the ignition delay period. Fuel 90, 766–772.
Saleh, H., Selim, M.Y., 2017. Improving the performance and emission characteristics of a diesel engine fueled by jojoba methyl ester-diesel-ethanol ternary blends. Fuel 207, 690–701.
Sendzikiene, E., Makareviciene, V., Janulis, P., 2006. Influence of fuel oxygen content on diesel engine exhaust emissions. Renew. Energy 31, 2505–2512.
Shahir, N.S., Masjuki, N.H., Kalam, M., Imran, A., Ashraful, A., 2015a. Performance and emission assessment of diesel–biodiesel–ethanol/bioethanol blend as a fuel in diesel engines: a review. Renew. Sustain. Energy Rev. 48, 62–78.
Shahir, S.A., Masjuki, H.H., Kalam, M.A., Imran, A., Ashraful, A.M., 2015b. Performance and emission assessment of diesel–biodiesel–ethanol/bioethanol blend as a fuel in diesel engines: a review. Renew. Sustain. Energy Rev. 48, 62–78.
Shanmugam, P., Sivakumar, V., Murugesan, A., Umarani, C., 2011. Experimental study on diesel engine using hybrid fuel blends. Int. J. Green Energy 8, 655–668.
Sharma, A., Murugan, S., 2015. Combustion, performance and emission characteristics of a DI diesel engine fuelled with non-petroleum fuel: a study on the role of fuel injection timing. J. Energy Inst. 88, 364–375.
Shehata, M., Razek, S.A., 2011. Experimental investigation of diesel engine performance and emission characteristics using jojoba/diesel blend and sunflower oil. Fuel 90, 886–897.
Shi, X., Pang, X., Mu, Y., He, H., Shuai, S., Wang, J., Chen, H., Li, R., 2006. Emission reduction potential of using ethanol–biodiesel–diesel fuel blend on a heavy-duty diesel engine. Atmos. Environ. 40, 2567–2574.
Shi, X., Yu, Y., He, H., Shuai, S., Wang, J., Li, R., 2005. Emission characteristics using methyl soyate–ethanol–diesel fuel blends on a diesel engine. Fuel 84, 1543–1549.
Solmaz, H., Ardebili, S.M.S., Calam, A., Yılmaz, E., İpci, D., 2021. Prediction of performance and exhaust emissions of a CI engine fueled with multi-wall carbon nanotube doped biodiesel-diesel blends using response surface method. Energy 227, 120518.
Solmaz, H., Calam, A., Yılmaz, E., Şahin, F., Ardebili, S.M.S., Aksoy, F., 2023. Evaluation of MWCNT as fuel additive to diesel–biodiesel blend in a direct injection diesel engine. Biofuels 14, 147–156.
Sperber, M., 2012. Diffuse Lung Disorders: A Comprehensive Clinical-Radiological Overview. Springer Science & Business Media.
Suresh, A., Babu, A.V., Balaji, B., Madhu Murthy, K., Ranjit, P.S., 2023. Experimental investigation of carbon nanotube additives on CRDI engine fueled with Chlorella vulgaris microalgae methyl ester and bio-ethanol blends: performance, emission and combustion characteristics. Biofuels 14, 551–563.
Szybist, J.P., Song, J., Alam, M., Boehman, A.L., 2007. Biodiesel combustion, emissions and emission control. Fuel Process. Technol. 88, 679–691.
Tong, D., Hu, C., Jiang, K., Li, Y., 2011. Cetane number prediction of biodiesel from the composition of the fatty acid methyl esters. J. Am. Oil Chem. Soc. 88, 415–423.
Towoju, O., 2022. Performance optimization of compression ignition engines: a review. Eng. Perspect. 2, 21–27.
Tsang, K., Zhang, Z., Cheung, C.S., Chan, T.L., 2010. Reducing emissions of a diesel engine using fumigation ethanol and a diesel oxidation catalyst. Energy Fuels 24, 6156–6165.
Turkcan, A., 2018. Effects of high bioethanol proportion in the biodiesel-diesel blends in a CRDI engine. Fuel 223, 53–62.
Venkatesan, H., Udhaya Kumar, V., Sivamani, S., Micha Premkumar, T., 2023. Evaluation of combustion, performance and emission characteristics of a diesel engine fuelled with diesel – jojoba biodiesel – n butanol with multi-walled carbon nanotube as fuel additive. Int. J. Ambient Energy 44, 1748–1766.
Venu, H., Veza, I., Selvam, L., Appavu, P., Raju, V.D., Subramani, L., Nair, J.N., 2022. Analysis of particle size diameter (PSD), mass fraction burnt (MFB) and particulate number (PN) emissions in a diesel engine powered by diesel/biodiesel/n-amyl alcohol blends. Energy 250, 123806.
Vergel-Ortega, M., Valencia-Ochoa, G., Duarte-Forero, J., 2021. Experimental study of emissions in single-cylinder diesel engine operating with diesel-biodiesel blends of palm oil-sunflower oil and ethanol. Case Stud. Therm. Eng. 26, 101190.
Wei, L., Cheung, C., Ning, Z., 2018. Effects of biodiesel-ethanol and biodiesel-butanol blends on the combustion, performance and emissions of a diesel engine. Energy 155, 957–970.
Yilmaz, N., Sanchez, T.M., 2012. Analysis of operating a diesel engine on biodiesel-ethanol and biodiesel-methanol blends. Energy 46, 126–129.
Yilmaz, N., Vigil, F.M., Donaldson, A.B., Darabseh, T., 2014. Investigation of CI engine emissions in biodiesel–ethanol–diesel blends as a function of ethanol concentration. Fuel 115, 790–793.
Yin, P., Prabhu, L., Saranya, S.N., Devanesan, S., Alsahi, M.S., Anderson, A., Praveenkumar, T.R., 2023. Effects of Scenedesmus dimorphus, spirulina biodiesel, hydrogen and nanoparticles fuel blends on mass burn fraction, emission, noise and vibration characteristics. Fuel 352, 129010.
Yoon, M., Choi, M., Kang, K., Oh, C., Park, Y., Choi, G., 2022. Effects of n-heptane/methane blended fuel on ignition delay time in pre-mixed compressed combustion. Energies 15 [Online].
Zhu, H., Bohac, S.V., Nakashima, K., Hagen, L.M., Huang, Z., Assanis, D.N., 2013. Effect of fuel oxygen on the trade-offs between soot, NOx and combustion efficiency in premixed low-temperature diesel engine combustion. Fuel 112, 459–465.
Zhu, L., Cheung, C.S., Zhang, W., Huang, Z., 2010a. Emissions characteristics of a diesel engine operating on biodiesel and biodiesel blended with ethanol and methanol. Sci. Total Environ. 408, 914–921.
Zhu, L., Cheung, C.S., Zhang, W., Huang, Z., 2011. Combustion, performance and emission characteristics of a DI diesel engine fueled with ethanol–biodiesel blends. Fuel 90, 1743–1750.
Zhu, Y., Murali, S., Cai, W., Li, X., Suk, J.W., Potts, J.R., Ruoff, R.S., 2010b. Graphene and graphene oxide: synthesis, properties, and applications. Adv. Mater. 22, 3906–3924.